Catalysis Letters Vol. 110, Nos. 3–4, September 2006 (© 2006)
DOI: 10.1007/s10562-006-0114-y

Effect of oxygen mobility in solid catalyst on transient regimes of catalytic reaction of methane partial oxidation at short contact times

S.I. Reshetnikov,* A.I. Lukashevich, G.M. Alikina, and V.A. Sadykov

Boreskov Institute of Catalysis RAS, Prospekt Ak. Lavrentieva 5, Novosibirsk, 630090, Russia

Received 1 May 2006; accepted 11 June 2006

Mathematical modeling of the effect of the oxygen mobility in a solid oxide catalyst on the dynamics of transients of fast catalytic reactions has been carried out. The analysis was based upon the redox mechanistic scheme with a due regard for diffusion of oxygen from the bulk of catalyst to its surface. Parameters of kinetic and mathematical models were selected via fitting of the experimental data for methane selective oxidation into syngas on 1.4%$Pt/Gd_{0.2}Ce_{0.4}Zr_{0.4}O_x$ catalyst. The range of the Thiele parameter (ϕ) where the oxygen bulk diffusion affects the most strongly reaction transients corresponds to $\phi \in [0.3 \div 7]$. For high-surface-area oxide catalysts, the bulk oxygen diffusion coefficients corresponding to this range of the Thiele parameter are in the range of$10^{-18} \div 10^{-13}$ cm^2/s.

KEY WORDS: oxygen mobility; methane partial oxidation; transient regimes.

1. Introduction

Diffusion of atoms and ions in the lattice of crystalline solids is known to be associated with the fluxes of point defects. As dependent upon the defect structure of solids, diffusion could involve jump of an atom/ion into the neighboring vacancy or interstitial position, cooperative cyclic movement of several atoms etc [1]. Diffusion in solid catalysts, first of all, oxygen diffusion in oxides, is a well known phenomenon having pronounced impact on the reaction dynamics. As the result, reaction rate is determined not only by the catalytic cycle by itself, but also by slower processes such as the oxygen diffusion in the catalyst affecting the state of its surface. All these processes, including steps of the reaction mechanism, are characterized by a certain duration, i.e. relaxation time. Variation of the reaction feed composition or temperature could affect in a different fashion the state of the catalyst surface, and, hence, the reaction rate leading to a complex dynamic behavior of a catalytic system. Hence, studies of the effect of the oxygen mobility in catalysts on their transient behavior in catalytic reactions are of a great importance, especially, for realization of processes in the unsteady-state regime, either in the absence of oxygen in the gas phase [2] or in its presence [3].

Traditionally, in the selective oxidation processes, transition metal oxides are used as catalysts or their components. Degree in which the lattice oxygen is involved in catalytic processes depends upon the bulk oxygen mobility and oxygen storage capacity. Thus, in the process of propylene oxidation on a layered Bi molybdate, oxygen ions from up to 500 monolayers could participate in the reaction products formation [4]. At the same time, for catalysts with a low mobility of the lattice oxygen (V–P–O catalyst, Fe–Sb–O etc), only 2–3 near-surface layers are involved in reaction [5, 6].

Complex oxides with fluorite-like structure, such as CeO_2–ZrO_2 system doped by rare-earth cations (Gd, La, Sm, Pr) [7–13] are now among the most broadly studied catalysts and supports. Doping of ceria–zirconia solid solution and promotion by supported platinum group metals allow to tune the bonding strength, mobility and reactivity of oxygen [14, 15]. These systems are of a great interest as catalysts of such important processes as car exhaust purification from CO, NO_x and CH_x, [16], natural gas conversion into syngas by its partial oxidation (POM), steam and dry reforming etc [17–19]. They possess very high activity in oxidation reactions, so equilibration of the feed is achieved at ms contact times [20, 21]. For POM, this appears to be caused by an efficient activation of CH_4 on supported Pt clusters as well as by the ability of fluorite-like oxides to accumulate a considerable amount of oxygen and provide its fast transfer from the bulk to the Pt-support interface where CH_x species formed on Pt particles are oxidized [22].

Due to a high reaction rate, the effect of the oxygen mobility on transient regime dynamics for fast catalytic reactions could differ considerable from that in traditional processes occurring at contact times $\sim$ seconds. In limits of a very high or very low oxygen mobility, this effect will be apparently very small. For catalysts based

*To whom correspondence should be addressed.
E-mail: reshet@catalysis.nsk.su

upon CeO_2 or CeO_2–ZrO_2, their lattice oxygen was shown to play an important role in transient regimes of methane oxidation [23–28]. In this respect, it is of interest to estimate the range of the lattice oxygen diffusion coefficients for which maximum deviations of the transient regimes from the steady state will be observed. This is primarily important for the molecular design of these nanostructured metal-oxide catalysts by control of the lattice oxygen mobility through variation of their chemical composition and defect structure.

This work primarily aims at theoretical analysis of the effect of the oxygen mobility in a solid catalyst on the dynamics of transients of fast catalytic reactions. Results were verified by comparison with the experimental data for dynamics of the methane selective oxidation into syngas studied in isothermal conditions.

2. Model formulation

Let us consider in general the mechanism of catalytic reaction accompanied by the oxygen diffusion from the bulk. A simplified scheme includes a stage of the dissociative oxygen adsorption (1) and a stage of the gas-phase reagent interaction with the active site leading to formation of a product P (2):

$$O_2 + 2Z \leftrightarrow 2ZO \tag{1}$$

$$\frac{A + nZO \rightarrow P + nZ}{A + (n/2)O_2 = P} \tag{2}$$

Here, Z centers are considered to include cations in some intermediate (an optimum one) oxidation state and/or coordination environment able to activate oxygen and/or retain the most reactive oxygen forms. These sites could be reduced more deeply by the reaction mixture components (or products) up to less reactive sites Z_R:

$$r)A + Z \rightarrow Z_R + AO \tag{3}$$

"Over-reduced" sites could be in turn reoxidized by the gas-phase oxygen:

$$o)O_2 + Z_R \rightarrow Z, \tag{4}$$

or by the "mobile " lattice oxygen:

$$s)[O]_S + Z_R \rightarrow Z \tag{5}$$

To reflect variation of the bulk oxide stoichiometry, this can be written as:

$$A + MeO_n = MEO_{n-1}$$
$$\tfrac{1}{2}O_2 + MeO_{n-1} = MeO_n$$
$$[O]_s + Meo_{n-1} = MeO_n$$

Hence, the reaction mechanism can be described by the next scheme:

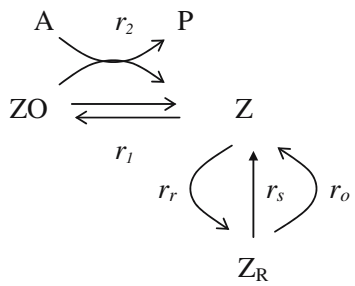

Equations for the rates of steps (1)–(5) can be written as:

$$\begin{aligned} r_1 &= k_1 Y_O \theta_Z - k_{-1}\theta_{ZO}; \quad r_2 = k_p Y_A \theta_{ZO}; \\ r_r &= k_r Y_A \theta_Z; \quad r_o = k_o Y_O \theta_R; \quad r_s = k_s \theta_R \sigma_s. \end{aligned} \tag{6}$$

where Y_A, Y_O – mole fractions of reagents A and O_2 in the gas phase; θ_Z, θ_{ZO}, θ_R – fractions of the active sites Z, ZO and Z_R, respectively; k_i – reaction rate constants for steps (1)–(5), c^{-1}; σ_s – "oxidation degree " of the near-surface layer.

Note that step (s) could be called "reaction" only from the formal point of view. In reality, it corresponds to filling the oxygen vacancies within the surface layer by mobile bulk oxygen species.

For simplicity of analysis of transient regimes of catalytic reaction, let us assume that reaction proceeds in the completely stirred tank reactor (CSTR), for which the mathematical model can be written as:

$$\begin{aligned} \frac{dY_i}{dt} &= \frac{1}{\tau_g}(Y_i^f - Y_i) + a\sum_{k=1}^{Nr} v_{ki} r_k(Y,\theta), \\ \frac{d\theta_j}{dt} &= \sum_{k=1}^{Nr} v_{kj} r_k(Y,\theta), \end{aligned} \tag{7}$$

with initial conditions:

$$t = 0: Y_i = Y_i^0, \theta_j = \theta_j^0, i = \overline{1, N_g}, j = \overline{1, N_d}.$$

and normalizing condition:

$$\theta_Z + \theta_{ZO} + \theta_R = 1.$$

Here, $\tau_g = V_g/w$; a is a parameter accounting for the total number of active sites; V_g is the reactor void volume, cm^3; w is the total gas flow rate, $cm^3 \cdot s^{-1}$; Y_i^f is the mole fraction of i-th component in the feed flow; N_r is the number of the reaction steps; N_g is the number of the reactants' components in the gas phase; N_d is the number of surface complexes; v_{ki} is a stoichiometric coefficient.

A degree of the catalyst surface oxidation, σ_s, is defined as the ratio of the oxygen content in the surface layer to its maximum level. It depends upon the rate of the oxygen ions diffusion from the bulk and the rate of the surface reduction [29, 30], as can be described by equation (8):

$$\frac{\partial\sigma}{\partial\tau} = \frac{1}{\varphi^2}\frac{\partial^2\sigma}{\partial\xi^2}, \tag{8}$$

with boundary conditions

$$\xi = 0 : \frac{d\sigma}{d\xi} = 0, \quad \xi = 1 : \frac{d\sigma}{d\xi} = -\varphi^2 \theta_R \sigma_s. \qquad (9)$$

where $\phi^2 = L^2 k_s / D$, so ϕ is an analogue of the Thiele parameter; D is an effective coefficient of the oxygen diffusion in the bulk of a catalyst; L is a typical size of the oxide crystallite; $\tau = k_s t$ is the dimensionless time; $\xi = l/L$ is the dimensionless coordinate in a crystallite.

The boundary condition on the crystallite surface depicts the fact that, on the one hand, the surface oxygen is consumed by the reaction, and, on the other hand, is replenished by the diffusion from the catalyst bulk.

As follows from equation (9), variation of the oxidation degree (σ) with the depth depends only on the Thiele parameter (ϕ), while its absolute value and the surface oxidation degree (σ_s) are also affected by dynamics of the active sites variation (θ).

The system of equations (7–9) was solved via the Runge-Kutt numerical integration, sweep method being applied for solving the diffusion equation in each integration step. This allowed to estimate the surface oxidation degree $\sigma_s = \sigma(\xi = 1)$ and an average integral oxidation degree of a catalyst:

$$\langle \sigma \rangle = \int_0^1 \sigma(t, \xi) d\xi.$$

To obtain quantitative characteristics of the effect of the oxygen mobility on the transients dynamics, numerical values of the constants of the mathematical (equations 7–9) and kinetic (equation 6) models are required. These constants were derived by analysis of the experimental data for methane oxidation into syngas at ms contact times of the complex ceria–zirconia oxide doped by Gd and promoted by supported Pt.

3. Experimental

In kinetic experiments, $1.4\%Pt/Gd_{0.2}Ce_{0.4}Zr_{0.4}O_x$ catalyst (specific surface area 130 m^2/g) was used. Single-phase Gd-doped ceria–zirconia fluorite-like complex oxide support was prepared via the polymerized precursor route following earlier described procedures [31, 32]. According to X-ray data, an average particle (domain) size was in the range of $20 \div 30$ nm [33]. The catalyst weight of 0.02 g (0.25–0.5 mm fraction) diluted with 0.1 cm^3 of a quartz sand was loaded into a flow quartz reactor (internal diameter 2.5 mm) forming a bed of 25 mm length. After sample pretreatment at 500 °C for 40 min in the flow of 1% O_2 in He, the reactor was purged by He, heated to required temperature (in the range of 650–880 °C) and then He flow was switched to the stream of 1% $CH_4 + 0.5\%$ O_2 in He (feed rate 7.2 l/h, contact time 5 ms). The diluted feed was used to ensure the isothermal profile in the catalyst bed. Variation of the outlet concentration of reagents and products (O_2, H_2O, CH_4, CO, CO_2 and H_2) up to the achievement of a steady-state was continuously monitored by an IR absorption PEM-2M gas analyzer additionally equipped with electrochemical and polarographic sensors for O_2 and H_2detection, a PC being used for the data acquisition and processing. In all experiments, the oxygen consumption was complete.

4. Results and discussion

Figure 1 presents the experimental data on the variation of methane conversion with time along with their fitting. Constants were selected by criteria of the best matching of experimental curves with the model ones. Thus, at 650 °C, the best fitting was achieved with the next combination of constants of the kinetic model (6): $k_1 = 10^4$, $k_{-1} = 1$, $k_p = 1500$, $k_r = 4.6$, $k_o = 0.47$, $k_s = 10^{-3}$, $n = 1$. Here, k_p determines the initial methane conversion, k_r – the curve slope, k_s – a shape of the curve, k_o – a steady-state conversion. The decrease of the Thiele parameter, and, hence, the intensity of the oxygen flux from the bulk to the surface, flattens the $x - t$ curve.

Though simplified kinetic model (vide supra) does not provide for existence of different types of surface active sites (Ce cations and Pt atoms), for the purpose of modeling the bulk oxygen mobility effect on the reaction transients, this is thought not to be of a great significance. This is primary determined by a much higher reactivity of Pt atoms both for methane [7, 22, 23] and

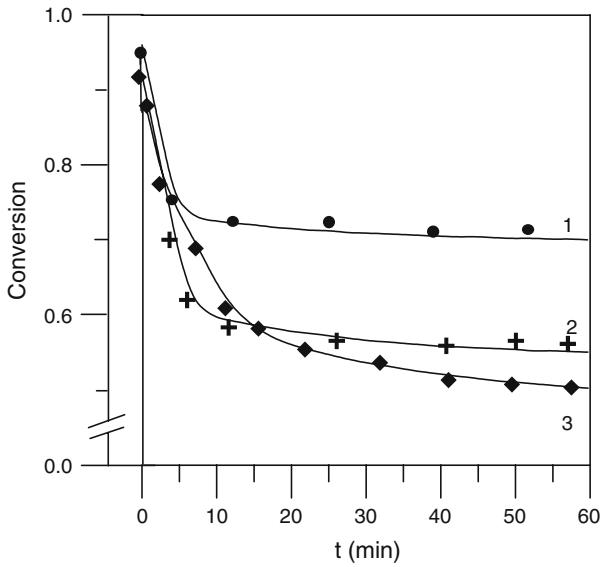

Figure 1. Dynamics of methane conversion after contact of oxidized $1.4\%Pt/Gd_{0.2}Ce_{0.4}Zr_{0.4}O_x$ catalyst with reaction mixture $1\%CH_4 + 0.5\%O_2$ in He at 880 °C (1), 750 °C (2) and 650 °C (3). Points denote experiment, lines denote modeling.

O_2 [10, 34] activation, so the surface steps are mainly controlled by the Pt reactivity, while supports mainly affects the relaxation features. This is also provided by a much higher rate of the surface diffusion as compared with the bulk diffusion [34].

The normalized reciprocal temperature dependences of constants of the kinetic model are given in figure 2 (R = 8.31 J/mol K). In studied temperature range (650–880 °C), the Thiele parameter varies rather moderately – from 1 to 0.45, its temperature dependence being determined by the k_s/D ratio. Since k_s characterizes the process of the oxygen atom jumping from the subsurface position into the surface vacancy, respective activation energy is expected to be not lower than the activation energy of the surface diffusion. According to Galdikas et al. [35], for Pt/ceria–zirconia catalyst, it is ~110 kJ/mol. This allows to estimate the activation energy of the bulk oxygen diffusion, which is ~170 kJ/mol. This value is rather close to the activation energy of the ionic conductivity in nanocrystalline ceria–zirconia system (~150 kJ/mol) estimated by Boaro et al. [36]. The bulk oxygen diffusion coefficient can be estimated as well. Thus, at 650 °C, ϕ = 1, which corresponds to L^2/D ratio = 1000. At L = 10 nm, the bulk diffusion coefficient will be equal to 10^{-15} cm^2/s. The rate constants at 650 °C were further used for analysis of the bulk oxygen mobility on the dynamics of transients.

Effect of the oxygen mobility in the lattice on the state of catalyst surface is mainly determined by the Thiele parameter $\phi^2 = L^2 k_s/D$. This effect is illustrated in figure 3 where time dependences of the crystallite oxidation degree at different ϕ values are given. Initially, only oxygen of near-surface layers takes part in methane oxidation. For low ϕ values (a fast bulk diffusion), the catalyst is reduced uniformly along the crystallite depth. For big ϕ values (a slow bulk diffusion), the lattice oxygen mobility is insufficient for the reoxidation of reduced surface. As the result, at bigger ϕ values, σ_s and methane conversion decline faster (figure 4).

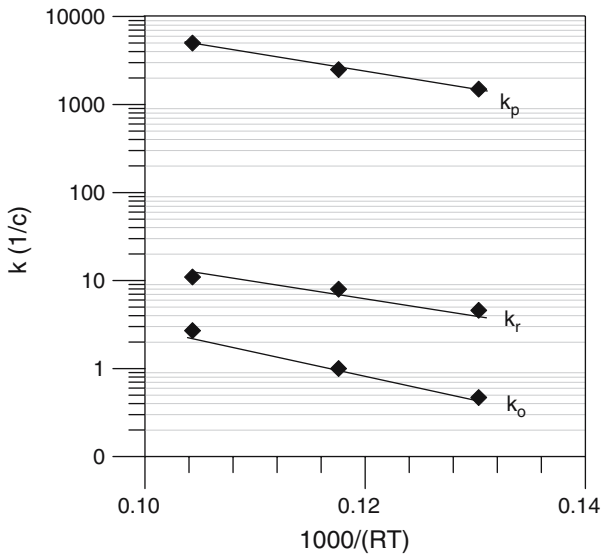

Figure 2. Normalized temperature dependence of reaction rate constants.

For the efficient control of the process start-up parameters, the bulk oxygen mobility should not determine the transients dynamics, i.e., the Thiele parameter should be small. This requires to define the range where the effect of diffusion is the highest. This can be best appreciated by the dependence of conversion and $\langle\sigma\rangle$ on the Thiele parameter (figure 5). Such a range is limited by the ϕ values varying from 0.3 to 7, i.e. $L^2/D \in (10^2 \div 5 \cdot 10^4)$.

Since Thiele parameter depends upon the L^2/D, this defines some set of L and D values. Hence, for estimation of D values, typical values of the oxide crystalline L in which diffusion occurs are to be known. They are determined by the real structure of the complex oxide (domain size and pore structure). In the first approximation, a single-domain crystallite could be considered as a wall separating either pores or disordered domain boundaries, where oxygen diffusion occurs much faster

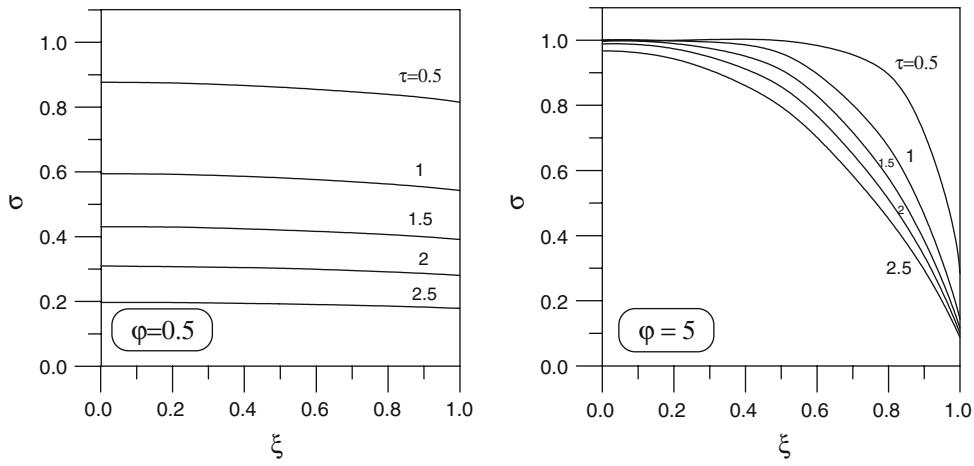

Figure 3. Dynamics of the crystallite oxidation degree variation at different Thiele parameters.

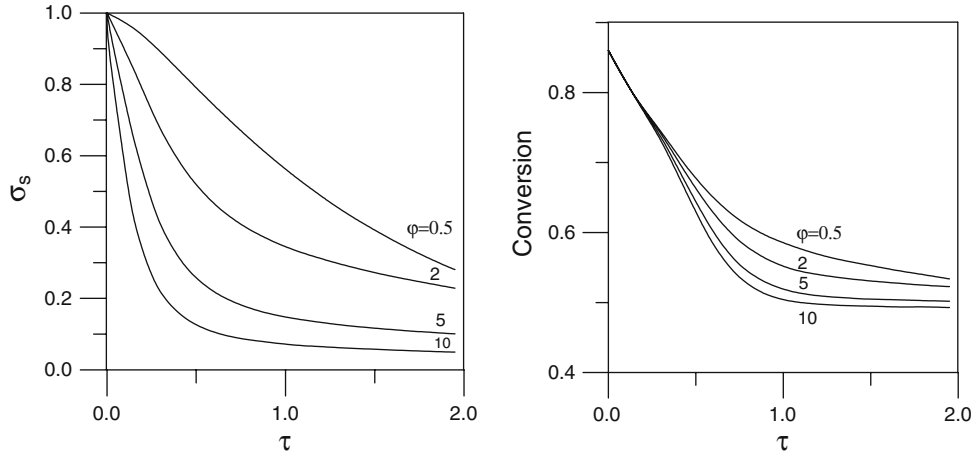

Figure 4. Time dependence of the surface oxidation degree of a crystallite at different values of Thiele parameter.

as compared with the crystallite bulk. In this case, L can be considered as a half of the wall thickness. For high-surface area complex oxides usually used as catalysts or their active components, typical values of domain size are in the range of 2–3 nm. This allows to estimate typical values of oxygen bulk diffusion coefficients being situated in the range of$10^{-18} \div 10^{-13}$ cm^2/s, which are in the range of known values for oxides [1, 37].

Table 1 presents some data for the oxygen diffusion parameters for single –crystalline and polycrystalline oxides of Ce, Zr and Pr. Due to effect of the samples real/defect structure as well as the applied method of

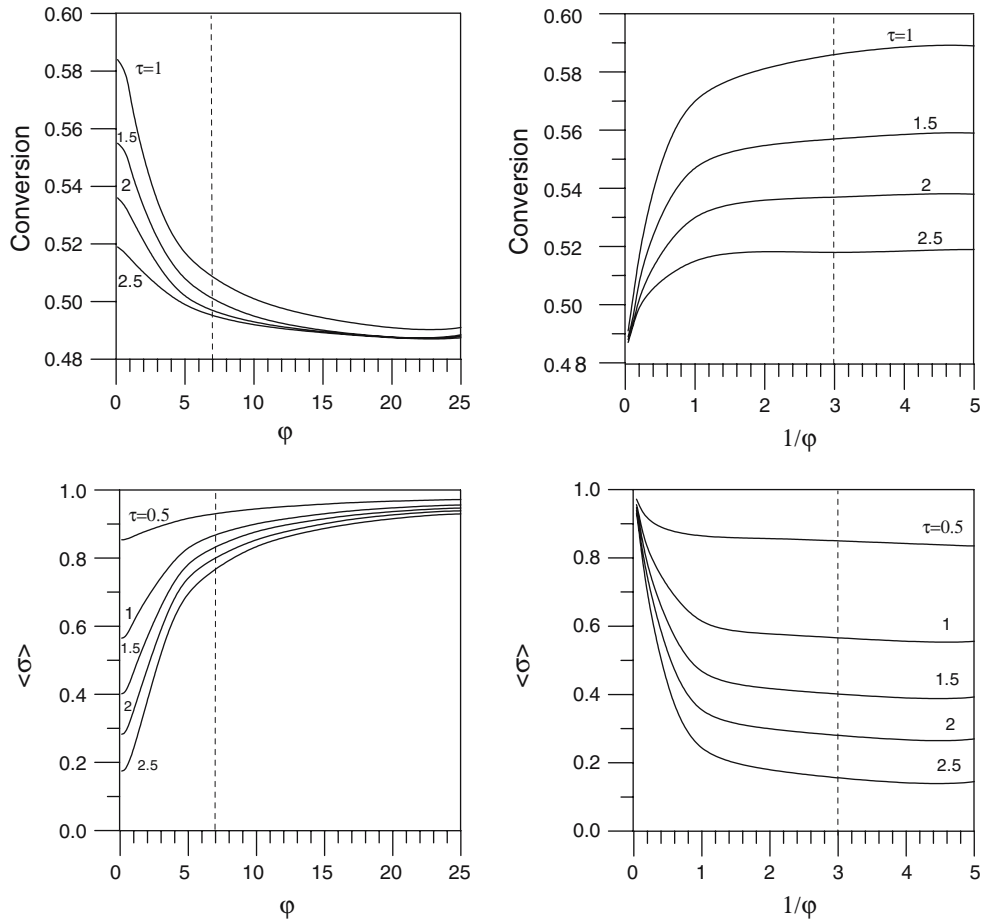

Figure 5. Dependence of the average catalyst oxidation degree ⟨σ⟩ and methane conversion on Thiele parameter at different temperatures.

Table 1
Bulk oxygen diffusion coefficients (cm^2/s), preexponential factor and activation energies (kJ/mol) for some oxides

Oxide	D_0	Q (kJ/mol)	D at 1000 °C	D at 500 °C	Comments
CeO_2	5.34×10^{2}	306	1.5×10^{-10}	1.2×10^{-18}	1150–1550 °C, Pure [38]
	9.55×10^{-5}	91	1.8×10^{-8}	6.8×10^{-11}	0.3%Gd (T = 1100–1300 °C)
	1.9×10^{-4}	104	1.0×10^{-8}	1.8×10^{-11}	850–1150 °C, (S), Isotope exchange [39]
	1.4×10^{-4}	89	3.1×10^{-8}	1.4×10^{-10}	(P)
	1.8×10^{-5}	73	1.8×10^{-8}	2.1×10^{-10}	(S)
	2.8×10^{-17}	15	6.8×10^{-18}	2.7×10^{-18}	300 °C, Isotope exchange [34]
Gd_2O_3	5.87×10^{-4}	120	7.0×10^{-9}	4.6×10^{-12}	737–1004 °C, Thermogravimetry [40]
Pr_7O_{12}	5.5×10^{-6}	77	3.8×10^{-9}	3.4×10^{-11}	735–865 °C, Isotope exchange [41]
	1.3×10^{-5}	80	6.8×10^{-9}	5.1×10^{-11}	830–930 °C
	5.5×10^{-6}	34	2.2×10^{-7}	2.8×10^{-8}	730–800 °C
	7.34×10^{-7}	64.5	1.6×10^{-9}	3.2×10^{-11}	1013–1153 °C,(S) Isotope exchange [42]
	6.28×10^{-7}	64.5	1.4×10^{-9}	2.7×10^{-11}	1013–1173 °C
	9.65×10^{-7}	64.5	2.2×10^{-9}	4.2×10^{-11}	1046–1193 °C
	6.29×10^{-7}	62.6	1.7×10^{-9}	3.7×10^{-11}	740–900 °C, (P)(S) Isotope exchange [43]
ZrO_2	9.7×10^{-3}	234	2.4×10^{-12}	1.5×10^{-18}	800–1000 °C, Radiometry [44]
	0.9×10^{-3}	130	1.1×10^{-8}	7.0×10^{-12}	334–470 °C, Pulse kinetic method [45]
	1.36×10^{-4}	119	1.8×10^{-9}	1.2×10^{-12}	875–1050 °C [46]

(S) – single crystalline material, (P) – polycrystalline material.
$D = D_o \exp(-E/RT)$.
Add Ce–Zr (below).

diffusion estimation, even for the same oxide, data vary considerably. However, in the temperature range of fast-occurring processes (such as methane selective oxidation into syngas etc.) realization, a lot of fluorite-like oxides have oxygen diffusion coefficients in the range of$10^{-18} \div 10^{-13}$ cm/s. Hence, for these oxides as supports, effect of the bulk oxygen diffusion during start-up conditions on the transients dynamics should be taken into account (figure 6).

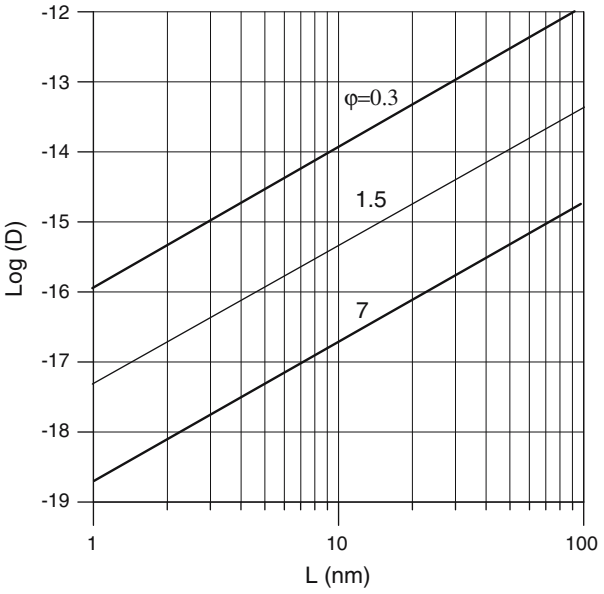

Figure 6. Range of oxygen diffusion coefficient values (cm^2/s) for crystallites of a different size where the lattice oxygen mobility affects transient dynamics.

To illustrate this feature, let us consider a mode of the main process parameters variation with time t for different ϕ values (figure 7). As ϕ increases (lattice oxygen mobility decreases), difference between the surface and bulk oxidation degree (σ_s and $\langle\sigma\rangle$) increases as well. Hence, at a low lattice oxygen mobility, reoxidation of the surface sites is hampered, thus being reflected in a fast decline of X and decreasing transient duration. On contrary, a high lattice oxygen mobility increases transient duration. As dependent upon the specific demands of the start-up process parameters control (to prevent the surface coking often caused by its excessive reduction, or its overheating leading to sintering of active component), these results are to be taken into account in design of the active components for monolithic catalysts of hydrocarbons selective oxidation into syngas at short contact times.

5. Conclusions

Mathematical modeling of the effect of the oxygen mobility in solid oxide catalyst on the dynamics of transients of fast catalytic reactions has been carried out. This analysis was based upon the redox mechanistic scheme with a due regard for diffusion of oxygen from the bulk of catalyst to its surface. Parameters of kinetic and mathematical models were selected via fitting of the experimental data for methane selective oxidation into syngas on 1.4%$Pt/Gd_{0.2}Ce_{0.4}Zr_{0.4}O_x$ catalyst at 650 °C and 5 ms contact time.

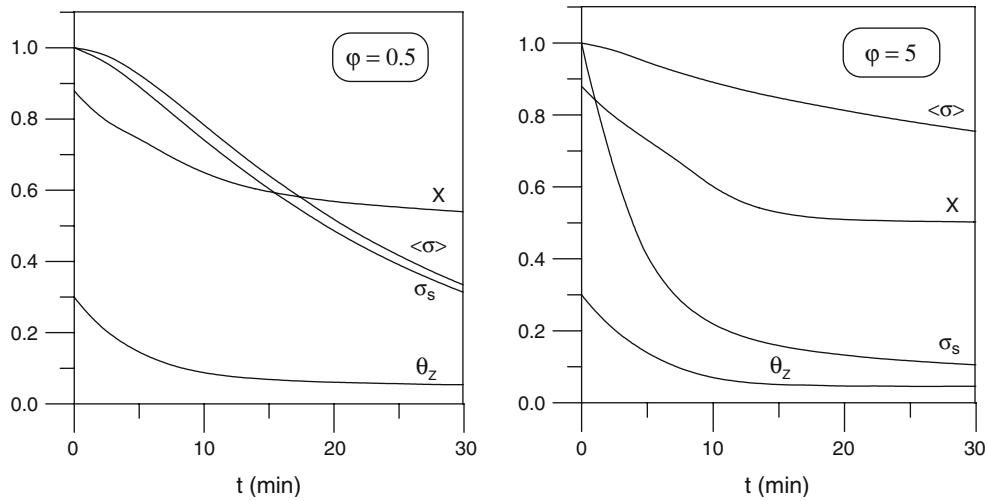

Figure 7. Dynamics of the reagent conversion (X), an average oxidation degree $\langle\sigma\rangle$ of the catalyst, surface oxidation degree (σ_s) and active sites concentration at different values of Thiele parameter.

Modeling revealed that there are two ranges of the Thiele parameter values when the bulk oxygen diffusion does not affect the dynamics of catalytic transient. The first one exists at $\phi < 0.3$, when the rate of the oxygen diffusion in the bulk is much higher than the rate of the catalyst reduction, while the second one corresponds to $\phi > 7$ where the oxygen mobility is low. Hence, the range of the Thiele parameter where the oxygen bulk diffusion affects the most strongly reaction transients corresponds to$\varphi \in [0.3 \div 7]$. For high-surface-area oxide catalysts, the bulk oxygen diffusion coefficients corresponding to this range of the Thiele parameter are $10^{-18} \div 10^{-13}$ cm^2/s.

Acknowledgment

This work is in part supported by RFBR-CNRS Project 05-03-34761.

References

[1] P. Kofstad, *Nonstoichiometry, Diffusion and Electrical Conductivity in Binary Metal Oxides* (Willey-Interscience, New-York, 1972).
[2] R.M. Contractor and A.E. Sleight, Catal. Today 1 (1987) 587.
[3] Yu.Sh. Matros, *Catalytic Processes under Unsteady State Conditions* (Elsevier, Amserdam, 1988).
[4] G.W. Keulks, J. Catal. 19 (1970) 232.
[5] G.W. Keulks and Lo. Man-Yin, J. Phys. Chem. 90 (1986) 4768.
[6] M. Misono, K. Mijamoto, K. Tsuji et al., In: New Developments in Selective Oxidation (Elsevier, Amsterdam, 1990, 573).
[7] V.A. Sadykov, T.G. Kuznetsova and G.M. Alikina et al., Catal. Today 93–95 (2004) 45.
[8] A. Heinzel, B. Vogel and P. Hubner, J. Power Sources 105 (2002) 202.
[9] S. Ahmed and M. Krumpelt, Int. J. Hydrogen Energy 26 (2001) 291.
[10] C. Descorme and D. Duprez, Appl. Catal. A: General 202 (2000) 231.
[11] V.S. Artunov and O.V. Krilov, Oxidation transformations of methane (M., Nauka, 1988) (in Russian).
[12] V. Krilov, Catal. Industry 2 (2002) 16(in Russian).
[13] S.S. Bharadwaj and L.D. Schmidt, J. Catal. 42 (1995) 109.
[14] M. Krumpelt, S. Ahmed, R. Kumar and R. Doshi, US Patent 6,110,861 (2000).
[15] H. Inaba and H. Tagawa, Solid State Ionics 83 (1996) 1.
[16] A. Trovarelly, Catal. Rev.-Sci. Eng. 38 (1996) 439.
[17] W.S. Dong, H.S. Roh, J.K. Jun and S.E. Park, Appl. Cat. A: General 236 (2002) 63.
[18] H.S. Roh, W.H. Dong, K.W. Jun and S.E. Park. Chem. Lett. (2001) 88.
[19] S.C. Tsang, J.B. Claridge and M.L. Green, Catal. Today 23 (1995) 3.
[20] M. Fathi, F. Monnet, Y. Schuurman, A. Holmen and C. Mirodatos, J. Catal. 190 (2000) 439.
[21] E.P.J. Mallens, J.H.B.J. Hoebnik and G.B. Marin, J. Catal. 167 (1997) 43.
[22] P. Pantu, K. Kim and G.R. Gavals, App. Catal. A 193 (2000) 203.
[23] V.A. Sadykov, T.G. Kuznetsova and S.A. Veniaminov et al., React. Kinet. Catal. Lett. 76 (2002) 83.
[24] T.G. Kuznetsova, V.A. Sadykov and E.M. Moroz et al., Stud. Surf. Sci. Catal. 143 (2002) 659.
[25] K. Otsuka, Ye. Wang and M. Nakamura, Appl. Catal. A 183 (1999) 317.
[26] K. Otsuka, T. Ushiyma and I. Yamanaka, Chem. Lett. (1993) 1517.
[27] M. Fathi, E. Bjorgum, T. Viig and O.A. Rokstad, Catal. Today 63 (2000) 489.
[28] Y. Zeng, S. Tamhankar and N. Ramprasad et al., Chem. Eng. Sci. 58 (2003) 577.
[29] N.M. Ostrovskii, Kinetic of catalyst deactivation. (M. Nauka, 2001). (in Russian).
[30] N.M. Ostrovskii and S.I. Reshetnikov, Chem. Eng. Journ. 107 (2005) 141.
[31] M.P. Pechini, U.S. Patent 3, 330, (1967) 697.
[32] T.G. Kuznetsova and V.A. Sadykov et al., Stud. Surf. Sci. Catal. 143 (2002) 659.
[33] V.A. Sadykov, Yu.V. Frolova-Borchert and N.V. Mezentseva et al., Mater. Res. Soc. Symp. Proc. 900E (2006) O10-04.
[34] F. Dong, A. Suda and T. Tanabe et al., Catalysis Today 93–95 (2004) 827.
[35] A. Galdikas, D. Duprez and C. Descorme, Appl. Surf. Sci. 236 (2004) 342.

[36] M. Boaro, F. Giordano, S. Recchia, V. Dal Santo, M. Giona and A. Trovarelli, Appl. Catal. B 52 (2004) 225.
[37] R. Freer, J. Mater. Sci. 15 (1980) 803.
[38] I.V. Vinokurov, Izv. Akad. Nauk SSSR 6 (1970) 31.
[39] F.H. Wohlbier, *Diffusion and Defect Data*, Vol. 4 (Diffusion Information Center, Cleveland, Ohio, 1970, p. 151).
[40] C.D. Wirkus, M.F. Berard and D.R. Wilder, J. Am. Ceram. Soc. 52 (1969) 456.
[41] J.R. Weber and L. Eyring, Ad. Chem. Phys. 21 (1971) 253.
[42] K.H. Lau and L. Eyring, CONF-730402-PL. NTIS. (Springfield, USA, 1973, p.184).
[43] K.H. Lau, D.L. Fox, S.N. Lin and L. Eyring, High. Temp. Sci. 35 (1073) 649.
[44] A. Madeyski and W.W. Smeltzer, Mat. Res. Bull. 3 (1966) 369.
[45] A.J. Rosenburg, J. Electrochem. Soc. 107 (1960) 795.
[46] C.J. Rosa and W.C. Hagel, Trans. AIME 242 (1968) 1293.